



| | |
|------------------|--|
| Title | In-situ biogas upgrading with H ₂ addition in an anaerobic membrane bioreactor (AnMBR) digesting waste activated sludge |
| Author(s) | Hafuka, Akira; Fujino, Sota; Kimura, Katsuki et al. |
| Citation | Science of the total environment, 828, 154573 https://doi.org/10.1016/j.scitotenv.2022.154573 |
| Issue Date | 2022-07-01 |
| Doc URL | https://hdl.handle.net/2115/91289 |
| Rights | © <2022>. This manuscript version is made available under the CC-BY-NC-ND 4.0 license https://creativecommons.org/licenses/by-nc-nd/4.0/ |
| Rights(URL) | https://creativecommons.org/licenses/by-nc-nd/4.0/ |
| Type | journal article |
| File Information | Revised manuscript for STOTEN_clean_100322.pdf |



1 **In-situ biogas upgrading with H₂ addition in an anaerobic membrane bioreactor**
2 **(AnMBR) digesting waste activated sludge**

3

4 Akira Hafuka,^{a,*} Sota Fujino,^a Katsuki Kimura,^a Kazuyuki Oshita,^b Naoya Konakahara,^c
5 Shigetoshi Takahashi^c

6

7 *^a Division of Environmental Engineering, Graduate School of Engineering, Hokkaido*
8 *University, North-13, West-8, Kita-ku, Sapporo 060-8628, Japan*

9 *^b Department of Environmental Engineering, Graduate School of Engineering, Kyoto*
10 *University, Katsura C1-3, Nishikyo-ku, Kyoto, 615-8540, Japan*

11 *^c Technology Center, Takuma Co., Ltd., 2-2-33 Kinrakuji-cho, Amagasaki, 660-0806, Japan*

12

13 *Corresponding author (A. Hafuka): E-mail address: ahafuka@eng.hokudai.ac.jp; Tel: +81-
14 11-706-6273.

15

16 **Abstract**

17 Biological in-situ biogas upgrading is a promising approach for sustainable energy-powered
18 technologies. This method increases the CH₄ content in biogas via hydrogenotrophic
19 methanogenesis with an external H₂ supply. In this study, an anaerobic membrane
20 bioreactor (AnMBR) was employed for in-situ biogas upgrading. The AnMBR was
21 operated in semi-batch mode using waste activated sludge as the substrate. Pulsed H₂
22 addition into the reactor and biogas recirculation effectively increased the CH₄ content in
23 the biogas. The addition of 4 equivalents of H₂ relative to CO₂ did not lead to appreciable
24 biogas upgrading, although the acetate concentration increased significantly. When 11
25 equivalents of H₂ were introduced, the biogas was successfully upgraded, and the CH₄
26 content increased to 92%. The CH₄ yield and CH₄ production rate were 0.31 L/g-VS_{input}
27 and 0.086 L/L/d, respectively. In this phase of the process, H₂ addition increased the acetate
28 concentration and the pH because of CO₂ depletion. Compared with a continuously-stirred
29 tank reactor, the AnMBR system attained higher CH₄ content, even without the addition of
30 H₂. The longer solid retention time (100 d) in the AnMBR led to greater degradation of
31 volatile solids. Severe membrane fouling was not observed, and the transmembrane
32 pressure remained stable under 10 kPa for 117 d of continuous filtration without cleaning of

33 the membrane. The AnMBR could be a promising reactor configuration to achieve in-situ
34 biogas upgrading during sludge digestion.

35

36 Keywords: Biomethanation; power to gas; anaerobic digestion; mesophilic; sewage sludge;
37 membrane fouling

38

39 **1. Introduction**

40 Wastewater treatment processes generate significant amounts of sludge, which places a
41 heavy burden on the environment (Ahmad et al., 2016). Dewatering followed by
42 incineration is widely used to treat sludge. Anaerobic digestion (AD) is another option to
43 treat sludge and it generates biogas. Biogas, which represents a potential energy source,
44 generally consists of methane (CH₄) and carbon dioxide (CO₂). The CH₄ and CO₂ contents
45 of biogas range from 40%–75% and from 25%–60%, respectively (Ryckebosch et al.,
46 2011). This insufficient CH₄ content makes it difficult to use the biogas directly as a bio-
47 natural gas; therefore, biogas upgrading, i.e., increasing the CH₄ content in biogas, is often
48 conducted (Nguyen et al., 2021; Sun et al., 2015). The obtained biogas with higher CH₄
49 content (>90%) can be used as vehicle fuel or natural gas (Deng and Hagg, 2010). Biogas

50 upgrading methods can be categorized as physical, chemical, or biological technologies
51 (Angelidaki et al., 2018), and some physical and chemical technologies are now
52 commercially available. Physical strategies, such as water scrubbing, pressure swing
53 adsorption, and membrane separation remove CO₂ from the biogas to increase its relative
54 CH₄ content; therefore, these physical techniques release CO₂ into the atmosphere (Fu et
55 al., 2021). Chemical absorption using amines has also been applied to remove CO₂ from
56 biogas; however, this method requires energy-intensive regeneration of the amine solution
57 (Ardolino et al., 2021). In contrast to absorption technologies, chemical reactions can
58 convert CO₂ into CH₄ using catalysts and an external H₂ source via the Sabatier reaction
59 (CO₂ + 4H₂ → CH₄ + 2H₂O). However, chemical reactions have disadvantages, including
60 the high reaction temperature (~300 °C) (Xia et al., 2016). Biological technologies that
61 convert CO₂ to CH₄ via hydrogenotrophic methanogenesis (CO₂ + 4H₂ → CH₄ + 2H₂O)
62 have attracted significant attention in recent years owing to their mild operational
63 conditions (i.e., low pressure and temperature) (Angelidaki et al., 2018; Fu et al., 2021; Lai
64 et al., 2021). Biological technologies can be further categorized as in-situ, ex-situ, or
65 hybrid-type biogas upgrading (Angelidaki et al., 2018; Zhao et al., 2021). In contrast to the
66 ex-situ and hybrid methods, the in-situ approach can achieve biogas generation and

67 upgrading in a single reactor by supplying H₂ directly to the anaerobic digester.

68

69 The power-to-gas strategy has also contributed to the increased attention regarding
70 biological biogas upgrading (Thema et al., 2019). This approach focuses on converting
71 surplus electricity from renewable energy sources (e.g., wind and solar energy) to gas fuel,
72 which is relatively easier to store and transport. Dihydrogen gas can be generated from the
73 electrolysis of water using surplus electricity. In general, further conversion of H₂ to CH₄ is
74 desirable because the volumetric energy density of H₂ is relatively low, and current
75 infrastructure can be used to store, transport, and use CH₄ (Götz et al., 2016). Therefore, in-
76 situ biogas upgrading with H₂ addition has been studied using batch tests (Luo et al., 2012;
77 Wang et al., 2016), continuously-stirred tank reactors (CSTRs) (Bassani et al., 2015; Jensen
78 et al., 2018; Zhu et al., 2019), and up-flow anaerobic sludge blankets (Bassani et al., 2016;
79 Park et al., 2021; Xu et al., 2020).

80

81 Anaerobic digestion of sludge enables biogas generation, while also reducing the volume of
82 sludge and destroying pathogens (Appels et al., 2008). However, the quality of effluent is
83 generally poor because of the low growth rates of anaerobic microorganisms and washout

84 of these microorganisms from the digester. To solve these problems, anaerobic membrane
85 bioreactors (AnMBRs) have been applied for sludge digestion (Abdelrahman et al., 2020).
86 An AnMBR comprises a system that couples membrane filtration with anaerobic treatment.
87 The distinguishing feature of AnMBRs involves the decoupling of hydraulic retention time
88 and solid retention time (Skouteris et al., 2012), which can prolong the SRT without
89 simultaneously extending the HRT following solid-liquid separation with membranes.
90 Therefore, AnMBRs generate higher-quality effluent than conventional CSTRs because the
91 membrane removes suspended solids (SS). Additionally, anaerobic microorganisms can be
92 retained inside the digester. Deschamps et al. (2021) have recently reported in-situ biogas
93 upgrading with H₂ addition in an AnMBR treating industrial wastewater. However, in-situ
94 biogas upgrading in an AnMBR configuration has not yet been applied for sewage sludge.
95 Therefore, the objective of the current study was to achieve in-situ biogas upgrading in an
96 AnMBR digesting sewage sludge. Waste activated sludge (WAS) was used as the substrate,
97 and the WAS digestion and biogas upgrading performance of the AnMBR system were
98 investigated. We tested the hypothesis that the amount of H₂ added would be a key factor
99 for in-situ biogas upgrading in the AnMBR.

100

101 **2. Materials and Methods**

102 *2.1 Reactor setup*

103 Figure 1 shows a schematic diagram of the AnMBR experimental apparatus, which
104 comprised a jar fermenter (BMS-03NP4, Biott Corporation, Tokyo, Japan) and an external
105 membrane unit. The external cross-flow configuration was selected to mitigate membrane
106 fouling (Hafuka et al., 2019). A vessel with a working volume of 2.37 L was continuously
107 mixed with a stirrer at 40 rpm. The temperature was held constant at 37 °C (i.e., mesophilic
108 conditions) with a heating jacket. The external membrane unit had a working volume of 0.1
109 L, and the unit contained a polyvinylidene fluoride hollow fiber microfiltration (MF)
110 membrane (Microza®, Asahi Kasei Corp., Tokyo, Japan). The total effective area of the
111 membrane was 0.0016 m², the inner diameter of each membrane fiber was 2.6 mm, and the
112 pore size of the membrane was 0.1 µm. The vessel was inoculated with seed sludge (2.16
113 L) obtained from a full-scale mesophilic digester in a sewage treatment plant. The
114 concentrations of total solids and volatile solids of the seed sludge were 13.1 g/L and, 8.9
115 g/L, respectively. Before starting the reactor operation, air in the reactor was purged with
116 N₂ gas. The WAS fed into the AnMBR was obtained from another full-scale sewage
117 treatment plant using a conventional activated sludge process. Raw WAS was screened

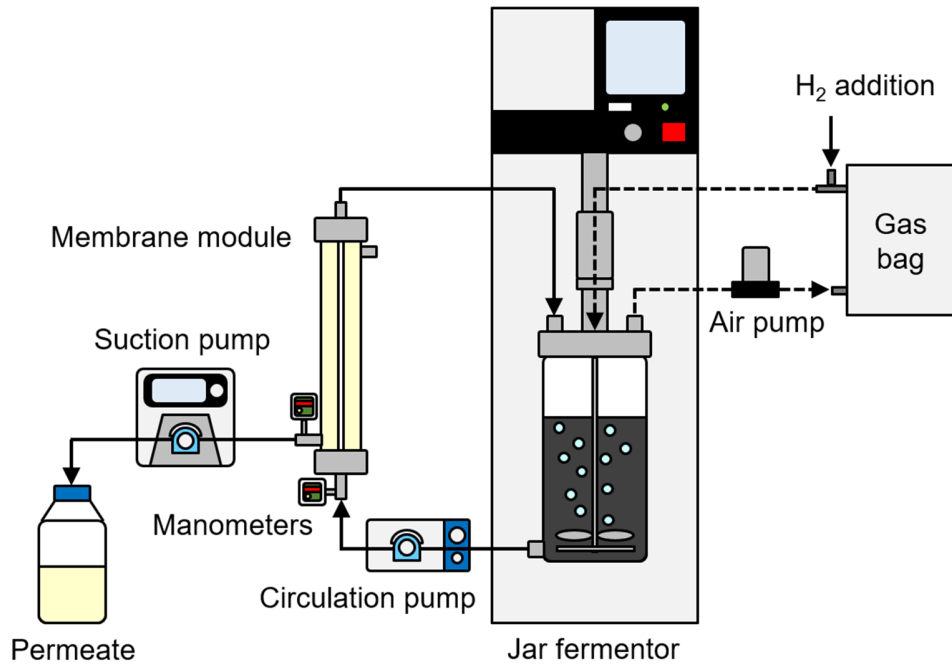
118 through a 1 mm mesh screen, and then the supernatant was removed to thicken the sludge.
119 The AnMBR was operated in semi-batch mode. Sludge feeding (0.21–0.57 L) and sludge
120 withdrawal (0.16–0.57 L) were performed manually once per week. The digested sludge
121 was circulated continuously using a peristaltic pump, and membrane filtration of the
122 digested sludge was performed at a constant cross-flow velocity of 0.5 m/s. This cross-flow
123 velocity is within the range of reported values (Abdelrahman et al., 2020). The digested
124 sludge was continuously filtered through the hollow fiber membrane, and the filtrate was
125 collected (i.e., inside-out filtration). The membrane flux was held constant by controlling
126 the filtrate flow rate with a peristaltic pump. The pressure inside and outside of the
127 membrane was measured daily using manometers, and the transmembrane pressure (TMP)
128 values were calculated from these data. The pH and oxidation-reduction potential (ORP) of
129 the digested sludge inside the fermenter were measured using an attached pH/ORP meter.
130 The biogas produced from the fermenter was stored in an aluminum gas bag, and the
131 volume of the biogas was measured using a wet gas meter (W-NK-0.5A, Shinagawa Co.,
132 Tokyo, Japan). The HRT and SRT of the reactor were controlled by changing the filtrate
133 flow rate and the sludge withdrawal volume according to Equations 1 and 2, respectively:

$$134 \quad \text{HRT (d)} = \frac{\text{Working volume of the reactor (L)}}{\text{Input of WAS (L/d)}} \quad (1)$$

135

136
$$\text{SRT (d)} = \frac{\text{Working volume of the reactor (L)}}{\text{Withdrawal of digested sludge (L/d)}} \quad (2)$$

137



138

139 **Figure 1.** Schematic diagram of the AnMBR.

140

141 *2.2 Reactor operating conditions*

142 The whole operating period of the reactor was 221 days, and it was divided into seven
143 separate phases, each involving distinct operational conditions (Table 1). The HRT and the
144 SRT values were selected based on a previous study (Abdelrahman et al., 2020). During
145 phase 1 (operation days 1–42), both the HRT and the SRT were set to 80 d (i.e., CSTR

146 mode without using the membrane module). Phase 1 was considered the acclimatization
147 period. The operation of the AnMBR began in phase 2 (operation days 42–102), during
148 which the HRT and SRT were set to 30 and 100 d, respectively. During phase 3 (operation
149 days 102–123), biogas was continuously re-circulated at 0.52 L/min between the fermenter
150 and gasbag using a diaphragm-type air pump (APN-10D3-W, IWAKI CO., LTD., Tokyo,
151 Japan). Biogas produced in the fermenter was passed through the gasbag and then re-
152 introduced into the fermenter through a diffuser. The diffuser, which had 12 pinholes ($\phi =$
153 0.6 mm), was located at the bottom of the vessel. Phase 4 (operation days 123–137)
154 involved in-situ biogas upgrading with added H₂ and biogas recirculation. Hydrogen gas
155 (99.99%) was collected from canned standard hydrogen gas (1020-11201, GL Sciences
156 Inc., Tokyo, Japan) and added to the gasbag five times per week (totally 0.54 L/week; see
157 supplementary material). During phase 5 (operation days 137–158), the H₂ addition rate
158 was increased to 1.50 L/week. To confirm the effect of AnMBR operation on CH₄ content
159 in biogas, CSTR operation without H₂ addition was continued during phase 6 (operation
160 days 158–179) and phase 7 (operation days 179–221).

161

162 **Table 1.** Operational conditions of each phase of the reactor.

| Phase No. | Operational mode | HRT (d) | SRT (d) | Filtration flux (LMH) | H ₂ addition (L/week) | Biogas recirculation rate (L/min) |
|-----------|------------------|------------|------------|--------------------------|-------------------------------------|--------------------------------------|
| 1 | CSTR | 80 | 80 | - | - | - |
| 2 | AnMBR | 33 | 107 | 1.29 | - | - |
| 3 | AnMBR | 30 | 102 | 1.46 | - | 0.52 |
| 4 | AnMBR | 30 | 98 | 1.38 | 0.54 | 0.52 |
| 5 | AnMBR | 29 | 98 | 1.46 | 1.50 | 0.52 |
| 6 | CSTR | 54 | 54 | - | - | 0.52 |
| 7 | CSTR | 29 | 29 | - | - | 0.52 |

163

164 2.3 Analytical methods

165 Selected physical and chemical properties of the WAS, membrane permeate, and digested
166 sludge were analyzed weekly. The concentrations of total solids (TS), volatile solids (VS),
167 chemical oxygen demand with potassium dichromate (COD_{Cr}), ammonium nitrogen (NH₄⁺-
168 N), and alkalinity were determined as previously described (Hafuka et al., 2019). The
169 concentrations of volatile fatty acids (VFAs; e.g., acetate, propionate, *i*-butyrate, *n*-butyrate,
170 *i*-valerate, and *n*-valerate) in the digested sludge were measured for samples after
171 centrifugation and filtration (0.20 μm; 25HP020AN, Toyo Roshi Kaisya, Ltd., Tokyo,
172 Japan) using a high-performance liquid chromatography system (LC-10AD, Shimadzu
173 Corporation, Kyoto, Japan) equipped with an electrical conductivity detector and a
174 stainless-steel-packed column with dimensions 0.3 m × 8.0 mm (Shim-pack SCR-102H;
175 Shimadzu Corporation, Kyoto, Japan). The CH₄, CO₂, and H₂ contents of the biogas were
176 determined using a gas chromatograph (GC-14B, Shimadzu Corporation, Kyoto, Japan)
177 equipped with a thermal conductivity detector and a 6.0 m × 3.0 mm stainless-steel-packed
178 column (Shincarbon St; Shinwa Chemical Industries, Ltd., Kyoto, Japan).

179

180 VS degradation efficiency was calculated based on the VS mass balance in each phase.

181 Biogas production rate and biogas yield were calculated by using cumulative biogas
182 volume obtained in each phase. The CH₄ production rate and CH₄ yield were calculated by
183 using average CH₄ content in biogas obtained in each phase. The efficiency of the COD
184 rejection by the membrane was calculated according to Equation 3,

185 COD rejection efficiency of the membrane (%)

$$186 \quad = \frac{COD_{\text{digested sludge}} - COD_{\text{permeate}}}{COD_{\text{digested sludge}}} \times 100 \quad (3)$$

187

188 where $COD_{\text{digested sludge}}$ (i.e., total COD) and COD_{permeate} (i.e., soluble COD) are the COD
189 concentrations of the digested sludge and permeate (mg/L), respectively.

190

191 *2.4 Membrane cleaning*

192 Membrane cleaning was conducted after the 221-day operation of the reactor. The
193 membrane unit was removed from the AnMBR and the inside of the hollow fiber
194 membrane was washed with tap water to physically remove the cake foulant. The filtration
195 resistance of the membrane was determined by filtering tap water at a pressure of 70 kPa.
196 Filtration resistances before and after cleaning were compared with the filtration resistance
197 of the pristine membrane, which was measured prior to the reactor operation. The filtration

198 resistances of the membranes were obtained according to Equations 4:

$$199 \quad R = \frac{\text{TMP (Pa)}}{\mu (\text{Pa} \cdot \text{s}) \times J (\text{m}^3/(\text{m}^2 \cdot \text{s}))} \quad (4)$$

200

201 where R is the filtration resistance, μ is the viscosity of water, and J is the permeate flux.

202

203 *2.5 Statistical analysis*

204 Pearson correlation coefficients were calculated to identify the significance of a correlation

205 between two parameters. The t -test was applied to analyze the minimum and maximum

206 acetate concentration and CH_4 content; p -values less than 0.05 were regarded as significant.

207 These analyses were performed using Origin Pro 9.8 software.

208

209 **3. Results and Discussion**

210 *3.1 In-situ biogas upgrading in an AnMBR*

211 The average TS and VS concentrations of the WAS were 9.9 g/L (± 2.2 g/L) and 7.9 g/L (\pm

212 1.8 g/L), respectively (Table 2). The VS/TS ratio remained stable at approximately 80% (\pm

213 2%), and the average total COD (T-COD) concentration in the WAS reached 12.4 ± 3.2 g/L.

214

215 **Table 2.** Characteristics of the raw WAS (n = 30).

| Parameters (unit) | Values \pm Standard deviations |
|---------------------------------------|----------------------------------|
| TS (g/L) | 9.9 \pm 2.2 |
| VS (g/L) | 7.9 \pm 1.8 |
| VS/TS (%) | 80 \pm 2 |
| T-COD (g/L) | 12.4 \pm 3.2 |
| NH ₄ ⁺ (mg-N/L) | 18 \pm 11 |
| pH (-) | 6.8 \pm 0.2 |

216

217 Table 3 summarizes the performance of the reactor during each phase. The CH₄ content in
218 the biogas was 83.1% (\pm 3.9%) in phase 2. Biogas recirculation began in phase 3 to
219 investigate its effect on the CH₄ content in biogas. As a result, the CH₄ content did not
220 change with biogas recirculation (85.2 \pm 2.3% in phase 3). In phase 4, H₂ was introduced
221 into the reactor to achieve in-situ biogas upgrading. Dihydrogen gas was added such that a
222 4:1 stoichiometric ratio of H₂/CO₂ was obtained; the cumulative biogas volume and average
223 CO₂ content obtained in phase 3 were used to determine the added amount of H₂. It was
224 confirmed that H₂ did not remain in the biogas, but rather, it was consumed one day after

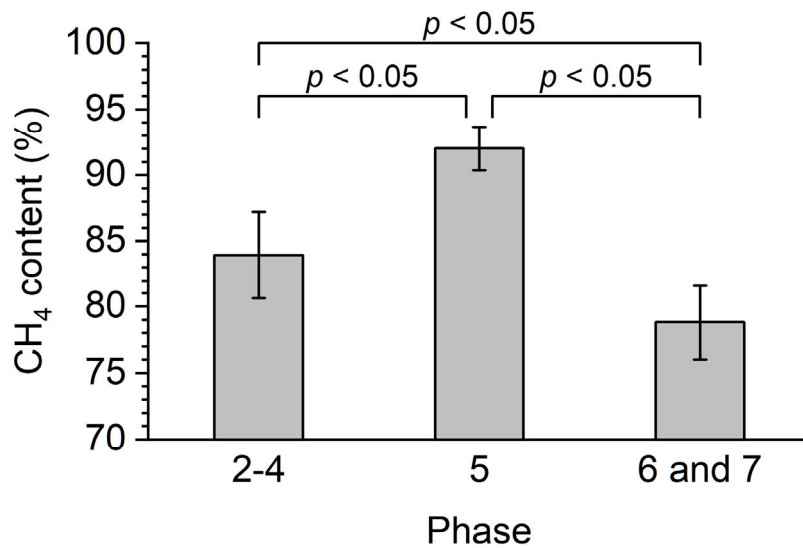
225 addition. As a result, the CH₄ content did not change (remained at $83.6 \pm 0.5\%$), indicating
226 that the biogas was not upgraded in phase 4. In phase 5, the amount of H₂ added was
227 increased to 11 molar equivalents relative to the CO₂ generated in the reactor. This quantity
228 was also determined based on the cumulative biogas volume and average CO₂ content
229 obtained in phase 4. In this phase, the CH₄ content increased significantly (to $92.0 \pm 1.6\%$)
230 compared with that detected in phases 2, 3, and 4 ($|t| = 4.41, p < 0.05$) (Figure 2). The CH₄
231 yield and CH₄ production rate were 0.31 L/g-VS_{input} and 0.086 L/L/d, respectively. H₂ did
232 not remain in the biogas samples. This result indicates that H₂ consumption rate was higher
233 than 0.13 L/L/d. Although high CH₄ content (i.e., 92%) was obtained in the present study,
234 the CH₄ production rate and H₂ consumption rate were lower than those reported in
235 previous studies probably due to the lower OLR (Alfaro et al., 2019; Lovato et al., 2017).
236 Energy balance analysis was conducted according to the Equations reported in previous
237 studies (Chen et al., 2019; Cheng et al., 2021; Xiao et al., 2018). In phase 5, the energy
238 production and net energy balance were 10.2 kJ/g-VS and 0.5 kJ/g-VS, respectively (see
239 supplementary material).

240

241 **Table 3.** WAS digestion performance of the system during each phase. ^a A biogas sample was not recovered.

| Phase | Organic loading rate (g-VS/L/d) | VS degradation (%) | Biogas yield (L/g-VS _{input}) | Biogas production rate (L/L/d) | CH ₄ content (%) | CH ₄ yield (L/g-VS _{input}) | CH ₄ production rate (L/L/d) |
|-------|------------------------------------|-----------------------|--|-----------------------------------|--------------------------------|---|--|
| 1 | 0.13 | 47 | 0.22 | 0.024 | - ^a | - | - |
| 2 | 0.21 | 65 | 0.29 | 0.076 | 83.1 ± 3.9 | 0.24 | 0.063 |
| 3 | 0.27 | 63 | 0.22 | 0.059 | 85.2 ± 2.3 | 0.19 | 0.050 |
| 4 | 0.26 | 55 | 0.33 | 0.087 | 83.6 ± 0.5 | 0.28 | 0.073 |
| 5 | 0.28 | 57 | 0.33 | 0.093 | 92.0 ± 1.6 | 0.31 | 0.086 |
| 6 | 0.29 | 44 | 0.30 | 0.084 | 80.3 ± 1.5 | 0.24 | 0.068 |
| 7 | 0.37 | 37 | 0.36 | 0.134 | 77.7 ± 3.0 | 0.28 | 0.104 |

242



243

244 **Figure 2.** Comparison in CH₄ content in biogas among operational phases.

245

246 *3.2 pH, ORP, alkalinity, and NH₄⁺ in an AnMBR*

247 The AnMBR investigated in this work achieved in-situ biogas upgrading following the

248 treatment of WAS, and the CH₄ content in the biogas reached 92% in phase 5 of the

249 process. There are very few studies regarding in-situ biogas upgrading using sewage sludge

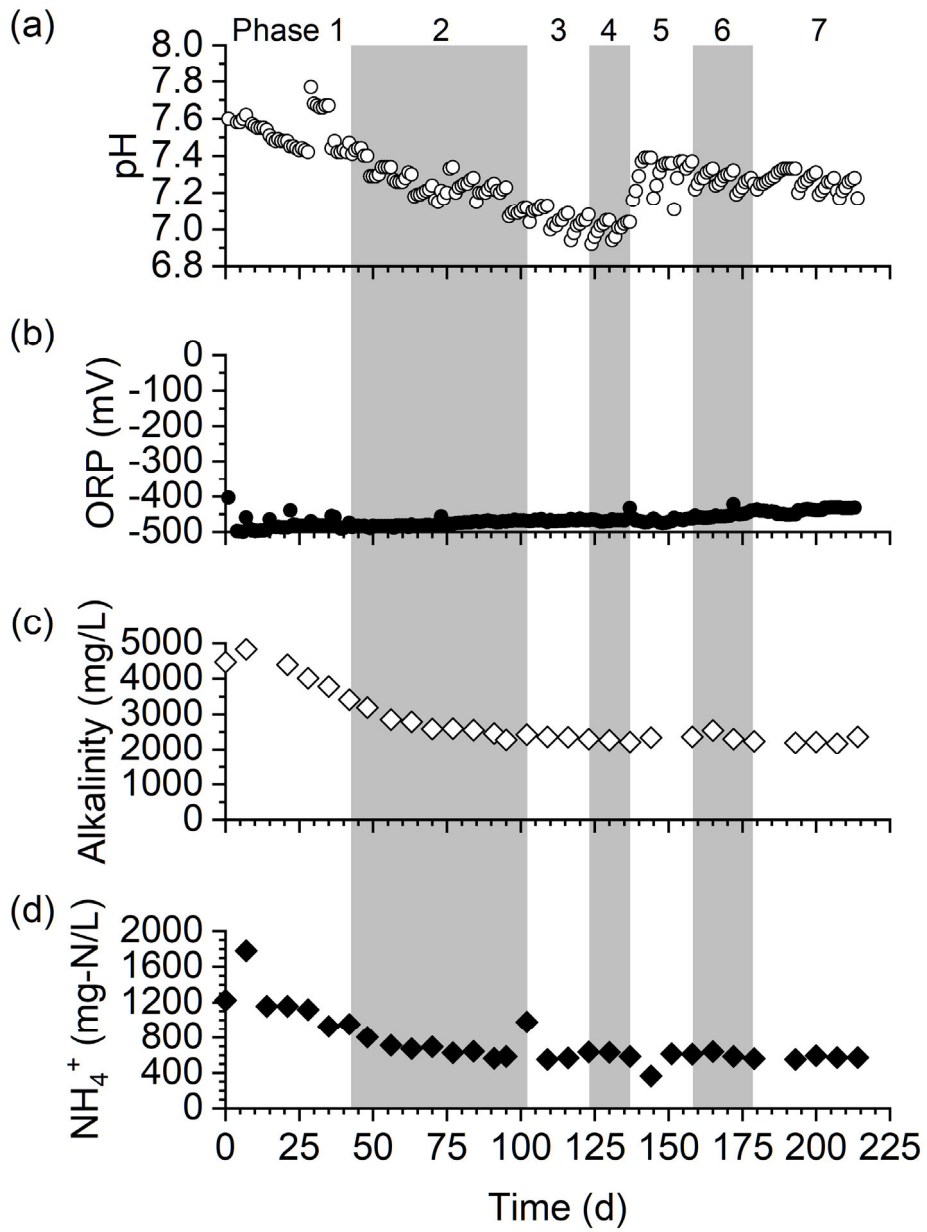
250 as the substrate (Alfaro et al., 2019; Lovato et al., 2017). Compared with those studies, the

251 system evaluated in this work obtained high CH₄ content. Furthermore, in phase 5, the CO₂

252 in the biogas was converted to CH₄ following the addition of H₂; this reduced the CO₂

253 content in the biogas to 8%. This also decreased the amount of CO₂ dissolved in the liquid

254 phase, which induced the increased pH in the reactor (Figure 3a). In one operational cycle
255 (i.e., one week), the pH decreased because of the WAS input, and then it gradually
256 increased within the cycle. Compared with the pH value measured in phases 2, 3, and 4, it
257 increased significantly to 7.3 ($|t| = 5.12, p < 0.01$) in phase 5 following the successful in-
258 situ biogas upgrading upon adding H₂ (see supplementary material). Although a rise in pH
259 occurred during phase 5, the pH values were in the range from 7.0–7.4, which was within
260 the ideal pH range for AD (Mao et al., 2015). The ORP was below -390 mV during
261 operation, confirming AD conditions in the fermenter (Figure 3b). The alkalinity gradually
262 decreased from 5000 mg/L at the start of operation and stabilized at around 2500 mg/L
263 during phases 3–7 (Figure 3c). The NH₄⁺ concentration was also stable at approximately
264 600 mg-N/L during phases 3–7 and remained below the inhibition level (Rajagopal et al.,
265 2013) (Figure 3d).
266



267

268 **Figure 3.** (a) pH, (b) ORP, (c) alkalinity, and (d) NH_4^+ concentration in the fermenter.

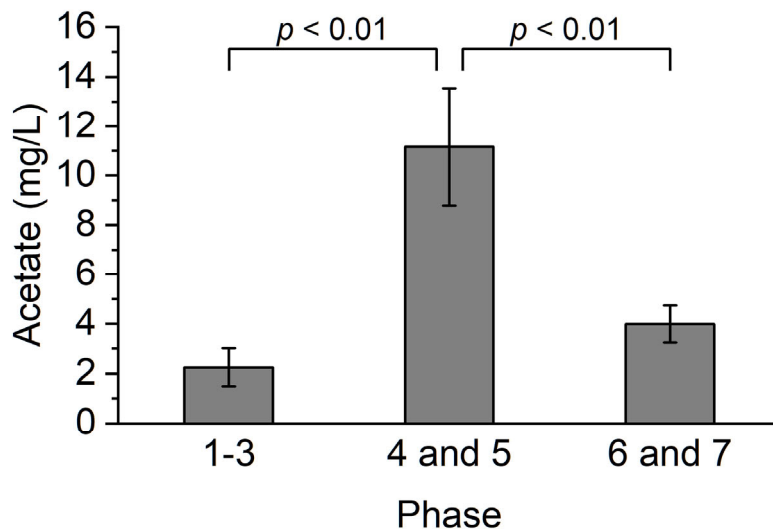
269

270 *3.3 Possible contributing factors for the successful in-situ biogas upgrading in an AnMBR*

271 Multiple factors contributed to the successful in-situ biogas upgrading demonstrated in this
272 study. First, the amount of H₂ added (i.e., 11 molar equivalents of H₂ relative to the CO₂
273 generated in the reactor) in phase 5 was optimal for in-situ biogas upgrading. The H₂/CO₂
274 ratio of 11:1 was consistent with results obtained by Agneessens et al. (2017). They
275 investigated the effect of H₂ addition on in-situ biogas upgrading in CSTRs and observed
276 that with a 10:1 ratio of H₂/CO₂, the CO₂ content in the headspace of the reactor decreased
277 to 7.9%. Second, pulsed H₂ addition in this study might be effective for in-situ biogas
278 upgrading. Agneessens et al. (2017) also found that pulsed H₂ addition increased the H₂
279 uptake rates and the activity of certain hydrogenotrophic methanogens. Third, although the
280 gas diffuser configuration and the biogas recirculation rate were not optimized in this study,
281 biogas recirculation through the gas diffuser could facilitate H₂ gas transfer to the liquid
282 phase. It is well known that the low gas-liquid mass transfer rate of H₂ is one of the limiting
283 factors in the in-situ biogas upgrading process because microorganisms use the dissolved
284 H₂ in the reactor (Bassani et al., 2016; Jensen et al., 2018; Park et al., 2021). Fourth, the
285 relatively low OLR (0.28 g-VS/L/d) in phase 5 may prevent process failure. H₂ addition
286 and in-situ biogas upgrading deplete the amount of dissolved CO₂ in the reactor, which

287 leads to the accumulation of VFAs (Mulat et al., 2017). Therefore, a high OLR might result
288 in significant VFA accumulation during in-situ biogas upgrading, which could lead to
289 reactor acidification and process deterioration (Franke-Whittle et al., 2014). Indeed, the
290 acetate concentration increased in phases 4 and 5 because of H₂ addition (Figure 4). The
291 acetate concentration remained stable at approximately 2.3 mg/L during phases 1, 2, and 3,
292 but then it increased significantly to 11 mg/L in phases 4 and 5 ($|t| = 7.40$, $p < 0.01$). No
293 other VFAs were detected in any of the analyzed samples. Compared with the acetate
294 concentrations in phases 4 and 5, those in phases 6 and 7 decreased significantly ($|t| = 5.85$,
295 $p < 0.01$) during CSTR operation without H₂ addition. Although H₂ was consumed and
296 acetate accumulated in phase 4, the CH₄ content did not increase (see Table 3). However,
297 the biogas yield increased from 0.22 L/g-VS_{input} in phase 3 to 0.33 L/g-VS_{input} in phase 4.
298 These results indicated that H₂ addition might inhibit acetate consumption and promote
299 acetate production by homoacetogens (Agneessens et al., 2017 and 2018; Liu et al., 2016;
300 Mulat et al., 2017).

301



302

303 **Figure 4.** Comparison in acetate concentration in the fermenter among operational phases.

304

305 *3.4 Comparison between AnMBRs and CSTRs without H₂ addition*

306 The CH₄ contents in phases 2 and 3 were high (83.1% and 85.2%, respectively) even if H₂
 307 was not added during the AnMBR mode of operation, relative to the general value (i.e., 40–
 308 75%). Therefore, the CSTR mode of operation without H₂ addition was used for phases 6
 309 and 7 to investigate the effect of the operational mode on the CH₄ content in biogas. As a
 310 result, the CH₄ contents in phases 6 and 7 were 80.3% (± 1.5%) and 77.7% (± 3.0%),
 311 respectively (see Table 3). Compared with the CH₄ contents in phases 2, 3, and 4, those in
 312 phases 6 and 7 were significantly lower ($|t| = 6.58, p < 0.05$) (see Figure 2). This result

313 indicated that the CH₄ content increased during AnMBR operation compared with CSTR
314 operation even if H₂ was not supplied to AnMBR. This suggested that it might be easier to
315 increase the CH₄ content in AnMBRs because the baseline CH₄ content was higher than
316 that in CSTRs.

317

318 There are three possible reasons for the higher CH₄ content in the AnMBR. First, the
319 membrane permeate might release dissolved inorganic carbon (i.e., dissolved CO₂ and
320 HCO₃⁻) outside of the fermenter, which would lead to higher CH₄ content (Yu et al., 2018).

321 In contrast to the CSTR mode of operation, this study involved continuous membrane
322 filtration in the AnMBR mode of operation during phases 2–5. Therefore, dissolved
323 inorganic carbon in the permeate may continuously flow outward, which would promote
324 further dissolution of CO₂ into the liquid phase in the fermenter. Because the Henry's
325 constant of CO₂ is higher than that of CH₄ (Sander et al., 2015), the CH₄ content in biogas
326 might show a relative increase in an AnMBR. Both the gradual reduction in pH during
327 phases 2–5 in the AnMBR and stable pH at approximately 7.3 during phases 6 and 7 in the
328 CSTR support this explanation (see Figure 3a). However, this could be a disadvantage of
329 AnMBRs because it is associated with a lost carbon source for conversion to CH₄.

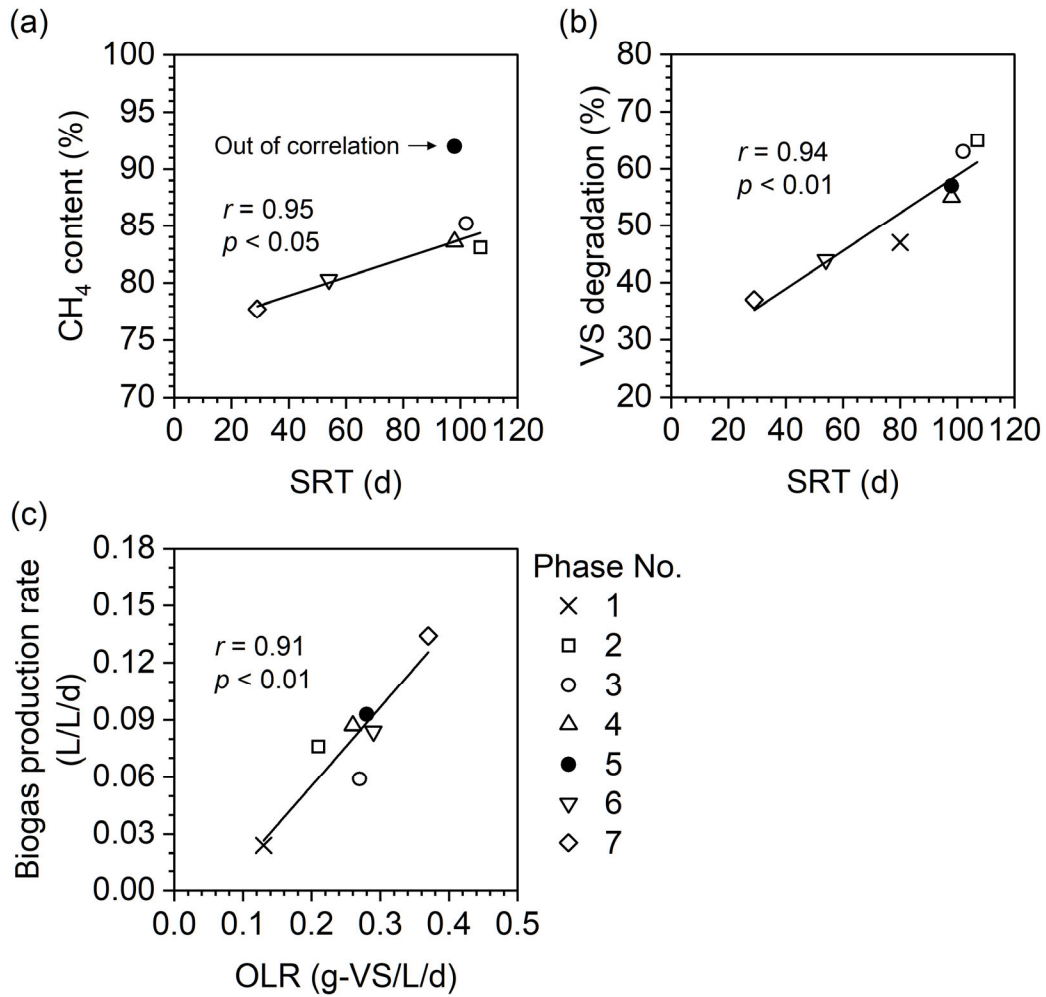
330

331 Second, the characteristics of the WAS substrate and the relatively long SRT in AnMBRs
332 may lead to higher CH₄ content in biogas. It is well known that proteins are the major
333 organic components of WAS (Xiao et al., 2017), and biogas obtained from the AD of WAS
334 has high CH₄ content (~71%) (Bougrier et al., 2007). In the present study, the SRT was
335 positively correlated with both the CH₄ content ($r = 0.95, p < 0.05$) and the VS degradation
336 efficiency ($r = 0.94, p < 0.01$) (Figure 5a and 5b). As shown in Figure 5a, the data point
337 obtained from phase 5 was out of correlation because the biogas was successfully upgraded
338 following H₂ addition. Compared with the CSTR mode, the AnMBR system developed in
339 this study achieved a higher VS degradation efficiency (see Figure 5b and Table 3).
340 Therefore, it is likely that the proteins in WAS were degraded well in the AnMBR because
341 of the longer SRT, which resulted in biogas with higher CH₄ content. The change in the
342 biogas production rate could be explained by the organic loading rate (OLR). A positive
343 correlation between the OLR and the biogas production rate ($r = 0.91, p < 0.01$) was
344 observed (Figure 5c). Therefore, the higher biogas production rate in phase 7 was a result of
345 the higher OLR (see Table 3).

346

347 Third, changes in the microbial community might affect the CH₄ content. Although the
348 microbial community was not investigated in the present study, Yu et al. (2016) reported
349 that hydrogenotrophic methanogenesis played a more important role in an anaerobic
350 dynamic membrane bioreactor, resulting in biogas with higher CH₄ content. Further
351 investigations are required to confirm these hypotheses.

352



353

354 **Figure 5.** Relationships between (a) SRT and CH₄ content in biogas, (b) SRT and VS

355 degradation efficiency, and (c) organic loading rate and biogas production rate.

356

357 *3.5 Performance of the membrane unit*

358 Although membrane fouling is an inevitable challenge in membrane-based treatment

359 processes (Meng et al., 2017; Wang et al., 2014), severe membrane fouling was not
360 observed in this study (Figure 6a). The TMP was stable under 10 kPa for 117 d of
361 continuous filtration without cleaning the membrane (phases 2–5). There are two reasons
362 for the successful mitigation of membrane fouling. One is that the reactor configuration
363 incorporated external cross-flow. There are two types of AnMBR configurations: external
364 cross-flow and submerged configurations (Abdelrahman et al., 2020). In external cross-
365 flow configurations, the membrane unit is outside of the digester, whereas in the submerged
366 configurations, membranes are immersed in the digester or external sludge tank. The high
367 shear force on the membranes in a cross-flow configuration can better control membrane
368 fouling (Abdelrahman et al., 2020). In addition, the use of an external membrane unit
369 outside the digester can provide ease of membrane maintenance since the head space of the
370 digester cannot be opened frequently in order to maintain anaerobic conditions. Although
371 cross-flow velocity of 0.5 m/s in the present study require additional energy (to power the
372 cross-flow pumps), they are proven to mitigate membrane fouling, and energy can be
373 recovered from the AD system in the form of biogas. Second, the relatively low filtration
374 flux (i.e., 1.25 LMH \approx 0.03 m/d) effectively prevented a drastic increase in the TMP in this
375 study. AnMBRs treating WAS have relatively long HRTs compared with aerobic or

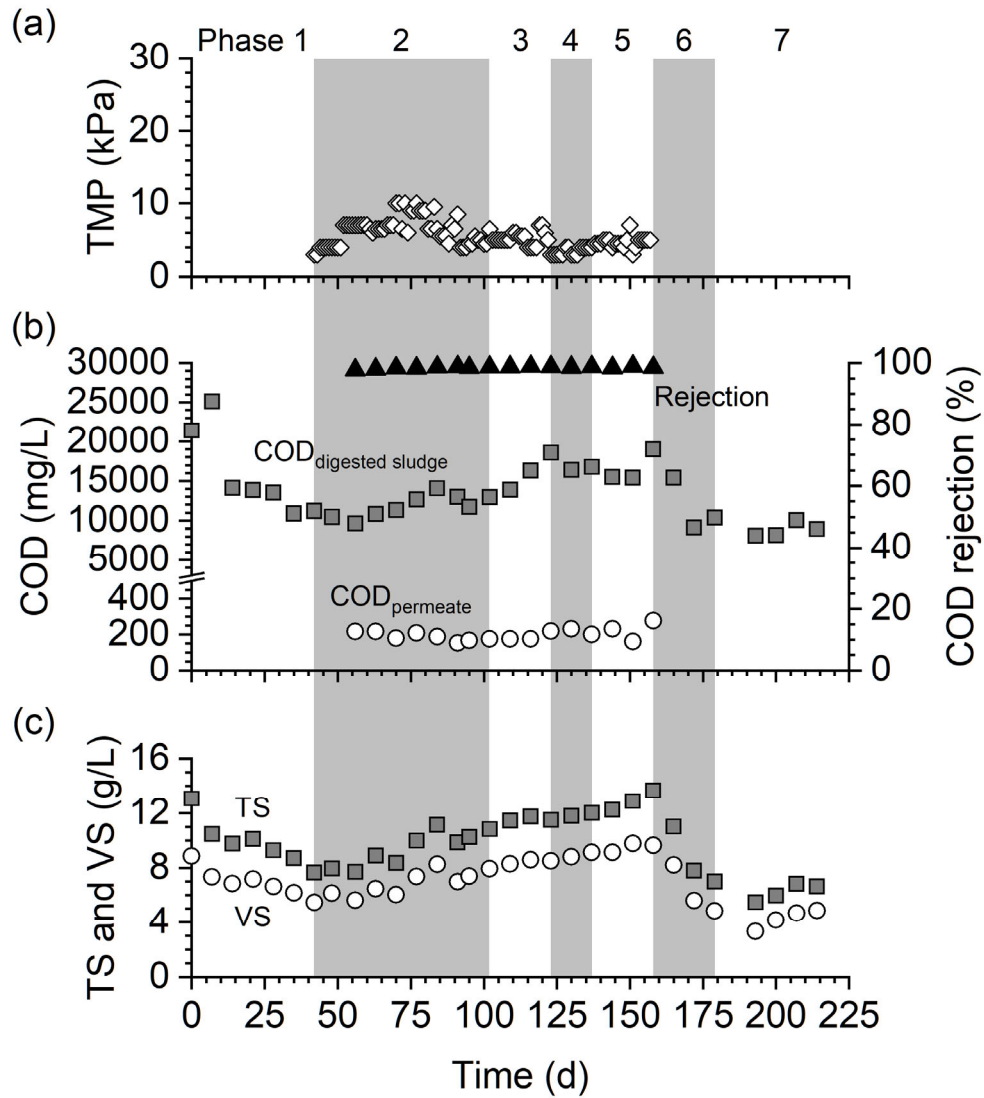
376 anaerobic membrane bioreactors treating low-strength wastewater. Therefore, a relatively
377 low flux is often sufficient for WAS digestion in AnMBRs, which could mitigate membrane
378 fouling (Hafuka et al., 2019).

379

380 In the AnMBR, the COD concentration in the membrane permeate stabilized at 210 mg/L
381 during phases 2–5, which suggested that the effluent quality was higher than that of a
382 conventional CSTR (Figure 6b). The COD concentration in the digested sludge was in the
383 range from 8000 to 25,200 mg/L, and it increased gradually from 10,500 to 19,000 mg/L
384 during phases 2–5, while membrane filtration continued. The same trend was observed for
385 the concentrations of TS and VS (Figure 6c). Overall, the efficiency of COD rejection by
386 the membrane was greater than 95%. This result was attributed to the membrane's highly
387 efficient rejection of suspended COD. The COD, TS, and VS concentrations in digested
388 sludge gradually increased during phases 2–5 because of the solid-liquid separation by the
389 membrane. In addition, these concentrations were higher than those in the WAS (see Table
390 2). These results suggested that the membrane thickened the WAS and helped retain the
391 digested sludge inside the reactor (Hafuka et al., 2016); these factors led to a higher content
392 of microbial biomass inside the reactor. In the present study, the AnMBR demonstrated a

393 high VS degradation efficiency compared to that of the CSTR because of the longer SRT
394 (100 d; see Figure 5b). This result originated from the distinctive feature of AnMBRs, i.e.,
395 the decoupling of the HRT and SRT. AnMBRs can prolong the SRT without simultaneously
396 extending the HRT, which shortens the overall treatment time and reduces the footprint of
397 the reactor (Cheng et al., 2021).

398



399

400 **Figure 6.** (a) TMP of the membrane unit over time; (b) COD concentrations of the digested

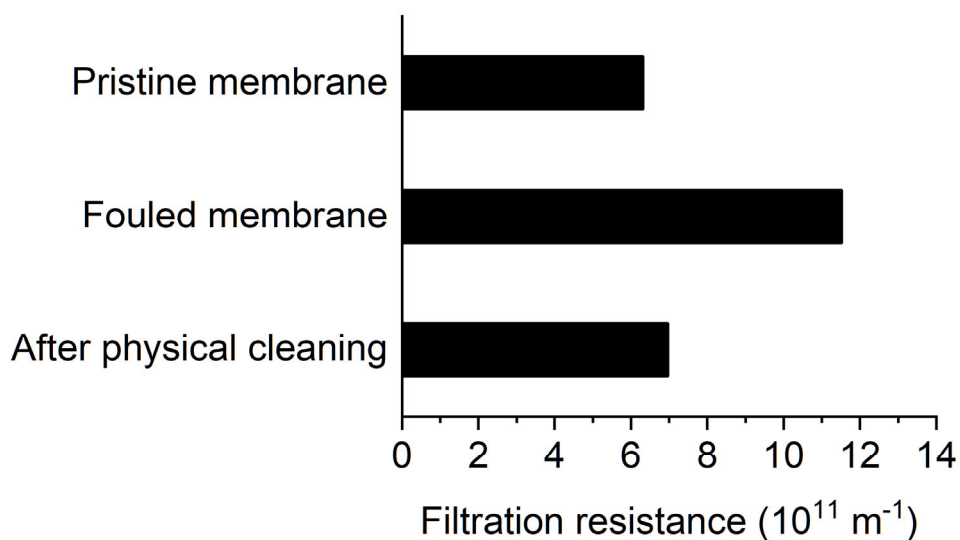
401 sludge and membrane permeate, as well as the efficiency of COD rejection by the

402 membrane; (c) TS and VS concentrations in the fermenter.

403

404 The filtration resistance of the pristine membrane was $6.3 \times 10^{11} \text{ m}^{-1}$ (Figure 7). The
405 resistance increased to $11.5 \times 10^{11} \text{ m}^{-1}$ due to membrane fouling after the 221-day operation
406 of the reactor. Hydraulic physical cleaning was effective in removing membrane foulants
407 and the resistance decreased to $7.0 \times 10^{11} \text{ m}^{-1}$. This result suggests that physically reversible
408 fouling had high contribution to the membrane fouling in the present study (Hafuka et al.,
409 2019).

410



411

412 **Figure 7.** Filtration resistances of the pristine membrane, the fouled membrane, and the
413 membrane after physical cleaning.

414

415 **4. Conclusions**

416 In this study, an AnMBR was employed to digest waste activated sludge in a semi-batch
417 mode, and the system demonstrated successful in-situ biogas upgrading. The CH₄ content
418 reached 92% when 11 equivalents of H₂ were added (relative to the CO₂ generated by the
419 fermenter). To our knowledge, this represents the first report detailing in-situ biogas
420 upgrading in an AnMBR digesting WAS. The addition of H₂ increased the acetate
421 concentration, and successful biogas upgrading led to an increased pH. Compared with the
422 CSTR mode of operation, the AnMBR mode of operation without added H₂ obtained higher
423 CH₄ contents. It was possible to conduct continuous membrane filtration of the digested
424 sludge over 117 d without cleaning the membrane. No appreciable rise in the TMP was
425 observed because of the low filtration flux and cross-flow filtration. The present study has
426 some limitations such as the low OLR and lacks an energy balance analysis. Further
427 research to solve these problems is now under way.

428

429 **Acknowledgments**

430 This research was financially supported by Takuma Co., Ltd., Japan. We also thank
431 Suzanne Adam, PhD, from Edanz (<https://jp.edanz.com/ac>) for editing a draft of this

432 manuscript.

433

434 **Appendix A. Supplementary Material**

435 Supplementary materials are available.

436

437 **References**

438 Abdelrahman, A.M., Ozgun, H., Dereli, R.K., Isik, O., Ozcan, O.Y., van Lier, J.B., Ozturk,

439 I., Ersahin, M.E., 2021. Anaerobic membrane bioreactors for sludge digestion: Current

440 status and future perspectives. *Crit. Rev. Environ. Sci. Technol.* 51, 2119–2157.

441 <https://doi.org/10.1080/10643389.2020.1780879>.

442 Agneessens, L.M., Ottosen, L.D.M., Andersen, M., Olesen, C.B., Feilberg, A., Kofoed,

443 M.V.W., 2018. Parameters affecting acetate concentrations during in-situ biological

444 hydrogen methanation. *Bioresour. Technol.* 258, 33–40.

445 <https://doi.org/10.1016/j.biortech.2018.02.102>.

446 Agneessens, L.M., Ottosen, L.D.M., Voigt, N.V., Nielsen, J.L., de Jonge, N., Fischer, C.H.,

447 Kofoed, M.V.W., 2017. In-situ biogas upgrading with pulse H₂ additions: The

448 relevance of methanogen adaption and inorganic carbon level. *Bioresour. Technol.* 233,

449 256–263. <https://doi.org/10.1016/j.biortech.2017.02.016>.

450 Ahmad, T., Ahmad, K., Alam, M., 2016. Sustainable management of water treatment sludge
451 through 3'R' concept. *J. Clean. Prod.* 124, 1–13.
452 <https://doi.org/10.1016/j.jclepro.2016.02.073>.

453 Alfaro, N., Fdz-Polanco, M., Fdz-Polanco, F., Diaz, I., 2019. H₂ addition through a
454 submerged membrane for in-situ biogas upgrading in the anaerobic digestion of sewage
455 sludge. *Bioresour. Technol.* 280, 1-8. <https://doi.org/10.1016/j.biortech.2019.01.135>.

456 Angelidaki, I., Treu, L., Tsapekos, P., Luo, G., Campanaro, S., Wenzel, H., Kougias, P.G.,
457 2018. Biogas upgrading and utilization: Current status and perspectives. *Biotechnol.*
458 *Adv.* 36, 452–466. <https://doi.org/10.1016/j.biotechadv.2018.01.011>.

459 Appels, L., Baeyens, J., Degreve, J., Dewil, R., 2008. Principles and potential of the
460 anaerobic digestion of waste-activated sludge. *Prog. Energy Combust. Sci.* 34,
461 755–781. <https://doi.org/10.1016/j.peccs.2008.06.002>.

462 Ardolino, F., Cardamone, G.F., Parrillo, F., Arena, U., 2021. Biogas-to-biomethane
463 upgrading: A comparative review and assessment in a life cycle perspective. *Renew.*
464 *Sust. Energ. Rev.* 139, 110588. <https://doi.org/10.1016/j.rser.2020.110588>.

465 Bassani, I., Kougias, P.G., Angelidaki, I., 2016. In-situ biogas upgrading in thermophilic

466 granular UASB reactor: key factors affecting the hydrogen mass transfer rate.
467 *Bioresour. Technol.* 221, 485–491. <https://doi.org/10.1016/j.biortech.2016.09.083>.

468 Bassani, I., Kougias, P.G., Treu, L., Angelidaki, I., 2015. Biogas Upgrading via
469 Hydrogenotrophic Methanogenesis in Two-Stage Continuous Stirred Tank Reactors at
470 Mesophilic and Thermophilic Conditions. *Environ. Sci. Technol.* 49, 12585–12593.
471 <https://doi.org/10.1021/acs.est.5b03451>.

472 Bougrier, C., Delgenes, J.P., Carrere, H., 2007. Impacts of thermal pre-treatments on the
473 semi-continuous anaerobic digestion of waste activated sludge. *Biochem. Eng. J.* 34,
474 20–27. <https://doi.org/10.1016/j.bej.2006.11.013>.

475 Chen, R., Wen, W., Jiang, H.Y., Lei, Z., Li, M.Z., Li, Y.Y., 2019. Energy recovery potential
476 of thermophilic high-solids co-digestion of coffee processing wastewater and waste
477 activated sludge by anaerobic membrane bioreactor. *Bioresour. Technol.* 274, 127–133.
478 <https://doi.org/10.1016/j.biortech.2018.11.080>.

479 Cheng, H., Li, Y.M., Hu, Y.S., Guo, G.Z., Cong, M., Xiao, B.Y., Li, Y.Y., 2021. Bioenergy
480 recovery from methanogenic co-digestion of food waste and sewage sludge by a high-
481 solid anaerobic membrane bioreactor (AnMBR): Mass balance and energy potential.
482 *Bioresour. Technol.* 326, 124754. <https://doi.org/10.1016/j.biortech.2021.124754>.

483 Deng, L.Y., Hagg, M.B., 2010. Techno-economic evaluation of biogas upgrading process
484 using CO₂ facilitated transport membrane. *Int. J. Greenh. Gas Control.* 4, 638–646.
485 <https://doi.org/10.1016/j.ijggc.2009.12.013>.

486 Deschamps, L., Imatoukene, N., Lemaire, J., Mounkaila, M., Filali, R., Lopez, M.,
487 Theoleyre, M.A., 2021. In-situ biogas upgrading by bio-methanation with an
488 innovative membrane bioreactor combining sludge filtration and H₂ injection.
489 *Bioresour. Technol.* 337, 125444. <https://doi.org/10.1016/j.biortech.2021.125444>.

490 Franke-Whittle, I.H., Walter, A., Ebner, C., Insam, H., 2014. Investigation into the effect of
491 high concentrations of volatile fatty acids in anaerobic digestion on methanogenic
492 communities. *Waste Manage.* 34, 2080–2089.
493 <https://doi.org/10.1016/j.wasman.2014.07.020>.

494 Fu, S.F., Angelidaki, I., Zhang, Y.F., 2021. In situ Biogas Upgrading by CO₂-to-CH₄
495 Bioconversion. *Trends Biotechnol.* 39, 336–347.
496 <https://doi.org/10.1016/j.tibtech.2020.08.006>.

497 Götz, M., Lefebvre, J., Mors, F., Koch, A.M., Graf, F., Bajohr, S., Reimert, R., Kolb, T.,
498 2016. Renewable Power-to-Gas: A technological and economic review. *Renew. Energ.*
499 85, 1371–1390. <https://doi.org/10.1016/j.renene.2015.07.066>.

500 Hafuka, A., Mashiko, R., Odashima, R., Yamamura, H., Satoh, H., Watanabe, Y., 2019.
501 Digestion performance and contributions of organic and inorganic fouling in an
502 anaerobic membrane bioreactor treating waste activated sludge. *Bioresour. Technol.*
503 272, 63–69. <https://doi.org/10.1016/j.biortech.2018.09.147>.

504 Hafuka, A., Mimura, K., Ding, Q., Yamamura, H., Satoh, H., Watanabe, Y., 2016.
505 Performance of anaerobic membrane bioreactor during digestion and thickening of
506 aerobic membrane bioreactor excess sludge. *Bioresour. Technol.* 218, 476–479.
507 <https://doi.org/10.1016/j.biortech.2016.06.124>.

508 Jensen, M.B., Kofoed, M.V.W., Fischer, K., Voigt, N.V., Agneessens, L.M., Batstone, D.J.,
509 Ottosen, L.D.M., 2018. Venturi-type injection system as a potential H₂ mass transfer
510 technology for full-scale in situ biomethanation. *Appl. Energy* 222, 840–846.
511 <https://doi.org/10.1016/j.apenergy.2018.04.034>

512 Lai, C.Y., Zhou, L., Yuan, Z., Guo, J., 2021. Hydrogen-driven microbial biogas upgrading:
513 Advances, challenges and solutions. *Water Res.* 197, 117120.
514 <https://doi.org/10.1016/j.watres.2021.117120>.

515 Liu, R.B., Hao, X.D., Wei, J., 2016. Function of homoacetogenesis on the heterotrophic
516 methane production with exogenous H₂/CO₂ involved. *Chem. Eng. J.* 284, 1196–1203.

517 <https://doi.org/10.1016/j.cej.2015.09.081>.

518 Lovato, G., Alvarado-Morales, M., Kovalovszki, A., Peprah, M., Kougias, P.G., Rodrigues,
519 J.A.D., Angelidaki, I., 2017. In-situ biogas upgrading process: Modeling and
520 simulations aspects. *Bioresour. Technol.* 245, 332–341.
521 <https://doi.org/10.1016/j.biortech.2017.08.181>.

522 Luo, G., Johansson, S., Boe, K., Xie, L., Zhou, Q., Angelidaki, I., 2012. Simultaneous
523 hydrogen utilization and in situ biogas upgrading in an anaerobic reactor. *Biotechnol.*
524 *Bioeng.* 109, 1088–1094. <https://doi.org/10.1002/bit.24360>.

525 Mao, C.L., Feng, Y.Z., Wang, X.J., Ren, G.X., 2015. Review on research achievements of
526 biogas from anaerobic digestion. *Renew. Sust. Energ. Rev.* 45, 540–555.
527 <https://doi.org/10.1016/j.rser.2015.02.032>.

528 Meng, F.G., Zhang, S.Q., Oh, Y., Zhou, Z.B., Shin, H.S., Chae, S.R., 2017. Fouling in
529 membrane bioreactors: An updated review. *Water Res.* 114, 151–180.
530 <https://doi.org/10.1016/j.watres.2017.02.006>.

531 Mulat, D.G., Mosbaek, F., Ward, A.J., Polag, D., Greule, M., Keppler, F., Nielsen, J.L.,
532 Feilberg, A., 2017. Exogenous addition of H₂ for an in situ biogas upgrading through
533 biological reduction of carbon dioxide into methane. *Waste Manage.* 68, 146–156.

534 <https://doi.org/10.1016/j.wasman.2017.05.054>.

535 Nguyen, L.N., Kumar, J., Vu, M.T., Mohammed, J.A.H., Pathak, N., Commault, A.S.,
536 Sutherland, D., Zdarta, J., Tyagi, V.K., Nghiem, L.D., 2021. Biomethane production
537 from anaerobic co-digestion at wastewater treatment plants: A critical review on
538 development and innovations in biogas upgrading techniques. *Sci. Total Environ.* 765,
539 142753. <https://doi.org/10.1016/j.scitotenv.2020.142753>.

540 Park, J.G., Kwon, H.J., Cheon, A.I., Jun, H.B., 2021. Jet-nozzle based improvement of
541 dissolved H₂ concentration for efficient in-situ biogas upgrading in an up-flow
542 anaerobic sludge blanket (UASB) reactor. *Renew. Energ.* 168, 270–279.
543 <https://doi.org/10.1016/j.renene.2020.12.019>.

544 Rajagopal, R., Masse, D.I., Singh, G., 2013. A critical review on inhibition of anaerobic
545 digestion process by excess ammonia. *Bioresour. Technol.* 143, 632–641.
546 <https://doi.org/10.1016/j.biortech.2013.06.030>.

547 Ryckebosch, E., Drouillon, M., Veruaeren, H., 2011. Techniques for transformation of
548 biogas to biomethane. *Biomass Bioenergy* 35, 1633–1645.
549 <https://doi.org/10.1016/j.biombioe.2011.02.033>.

550 Sander, R., 2015. Compilation of Henry's law constants (version 4.0) for water as solvent,

551 Atmospheric Chem. Phys. 15, 4399–4981. <https://doi.org/10.5194/acp-15-4399-2015>.

552 Skouteris, G., Hermosilla, D., Lopez, P., Negro, C., Blanco, A., 2012. Anaerobic membrane
553 bioreactors for wastewater treatment: A review. Chem. Eng. J. 198, 138–148.
554 <https://doi.org/10.1016/j.cej.2012.05.070>.

555 Sun, Q., Li, H.L., Yan, J.Y., Liu, L.C., Yu, Z.X., Yu, X.H., 2015. Selection of appropriate
556 biogas upgrading technology-a review of biogas cleaning, upgrading and utilization.
557 Renew. Sust. Energ. Rev. 51, 521–532. <https://doi.org/10.1016/j.rser.2015.06.029>.

558 Thema, M., Bauer, F., Sterner, M., 2019. Power-to-Gas: Electrolysis and methanation status
559 review. Renew. Sust. Energ. Rev. 112, 775–787.
560 <https://doi.org/10.1016/j.rser.2019.06.030>.

561 Wang, H., Zhang, Y.F., Angelidaki, I., 2016. Ammonia inhibition on hydrogen enriched
562 anaerobic digestion of manure under mesophilic and thermophilic conditions. Water
563 Res. 105, 314–319. <https://doi.org/10.1016/j.watres.2016.09.006>.

564 Wang, Z.W., Ma, J.X., Tang, C.Y.Y., Kimura, K., Wang, Q.Y., Han, X.M., 2014. Membrane
565 cleaning in membrane bioreactors: A review. J. Membr. Sci. 468, 276–307.
566 <https://doi.org/10.1016/j.memsci.2014.05.060>.

567 Xia, A., Cheng, J., Murphy, J.D., 2016. Innovation in biological production and upgrading

568 of methane and hydrogen for use as gaseous transport biofuel. *Biotechnol. Adv.* 34,
569 451–472. <https://doi.org/10.1016/j.biotechadv.2015.12.009>.

570 Xiao, B.Y., Qin, Y., Qu, J., Chen, H., Yu, P.F., Liu, J.X., Li, Y.Y., 2018. Comparison of
571 single-stage and two-stage thermophilic anaerobic digestion of food waste:
572 Performance, energy balance and reaction process. *Energy Convers. Manag.* 156,
573 215–223. <https://doi.org/10.1016/j.enconman.2017.10.092>.

574 Xiao, K.K., Chen, Y., Jiang, X., Seow, W.Y., He, C., Yin, Y., Zhou, Y., 2017. Comparison of
575 different treatment methods for protein solubilisation from waste activated sludge.
576 *Water Res.* 122, 492–502. <https://doi.org/10.1016/j.watres.2017.06.024>.

577 Xu, H., Wang, K.J., Zhang, X.Q., Gong, H., Xia, Y., Holmes, D.E., 2020. Application of in-
578 situ H₂-assisted biogas upgrading in high-rate anaerobic wastewater treatment.
579 *Bioresour. Technol.* 299, 122598. <https://doi.org/10.1016/j.biortech.2019.122598>.

580 Yu, D.W., Meng, X.S., Liu, J.B., Dian, L., Sui, Q.W., Zhang, J.Y., Zhong, H., Wei, Y.S.,
581 2018. Formation and characteristics of a ternary pH buffer system for in-situ biogas
582 upgrading in two-phase anaerobic membrane bioreactor treating starch wastewater.
583 *Bioresour. Technol.* 269, 57–66. <https://doi.org/10.1016/j.biortech.2018.08.072>.

584 Yu, H.G., Wang, Z.W., Wu, Z.C., Zhu, C.W., 2016. Enhanced waste activated sludge

585 digestion using a submerged anaerobic dynamic membrane bioreactor: performance,
586 sludge characteristics and microbial community. *Sci. Rep.* 6, 20111.
587 <https://doi.org/10.1038/srep20111>.

588 Zhao, J., Li, Y., Dong, R.J., 2021. Recent progress towards in-situ biogas upgrading
589 technologies. *Sci. Total Environ.* 800, 149667. [https://doi.org/](https://doi.org/10.1016/j.scitotenv.2021.149667)
590 [10.1016/j.scitotenv.2021.149667](https://doi.org/10.1016/j.scitotenv.2021.149667).

591 Zhu, X.P., Cao, Q., Chen, Y.C., Sun, X.Y., Liu, X.F., Li, D., 2019. Effects of mixing and
592 sodium formate on thermophilic in-situ biogas upgrading by H₂ addition. *J. Clean.*
593 *Prod.* 216, 373–381. <https://doi.org/10.1016/j.jclepro.2019.01.245>.